# Local Temperature Determination of Optically-Excited Nanoparticles and Nanodots

Michael T. Carlson,[1] Aurangzeb Khan,[2] and Hugh H. Richardson[1*]

[1]Department of Chemistry and Biochemistry, Ohio University, Athens, Ohio 45701 USA

[2]Biomimetic Nanoscience and Nanoscale Technology Program (BNNT), Ohio University, Athens, Ohio 45701 USA

[*]To whom correspondence should be addressed richards@helios.phy.ohiou.edu

## Supporting Information

### Characterization of heat generation.

The extinction from nanometer size structures is described by Mie theory.[48] For nanostructures embedded in a matrix of dielectric constant $\varepsilon_m$, when $\frac{2\pi\sqrt{\varepsilon_m}R_{NP}}{\lambda} \ll 1$, the electric dipole term in MIE theory dominates and the extinction cross section, $C_{ext}$, is given by equation S1,[49, 50] where ε' and ε" are the real and imaginary dielectric constants of the metallic nanostructure respectively and λ is the wavelength of light. Small nanostructures ($R_{NP} \leq 20$ nm) scatter little light and the extinction cross section is equal to the absorption cross section ($C_{abs}$). If the NP is embedded in a transparent matrix with thermal conductivity $k_m$, it can be shown (see below) that the maximum temperature at the NP surface is related to the amount of light absorbed with the steady-state temperature given by equation S2,[51] where $I_o$ is the light intensity.

$$C_{ext}(\lambda) = \frac{24\pi^2 R_{NP}^3 \varepsilon_m^{3/2}}{\lambda}\left[\frac{\varepsilon''}{(\varepsilon' + 2\varepsilon_m)^2 + (\varepsilon'')^2}\right] \quad \text{(S1)}$$

$$\Delta T_{\max}(\lambda) = \frac{6\pi R_{NP}^2 \varepsilon_m^{3/2} I_o}{k_m \lambda}\left[\frac{\varepsilon''}{(\varepsilon' + 2\varepsilon_m)^2 + (\varepsilon'')^2}\right] = \frac{C_{abs}(\lambda) I_o}{4\pi k_m R_{NP}} \quad \text{(S2)}$$

The attenuation of light through a medium of path length d decrease exponentially and is given by equation S3 where $I/I_o$ is the transmittance, $C_{ext}$ is the extinction cross section, and N is the number density giving the number of nanoparticles (NP) in a unit volume. N and d can be combined to give S, the number of NPs per unit area.

$$T_\lambda = \frac{I}{I_o} = \exp(-NC_{ext}d) = \exp(-C_{ext}S) \quad \text{(S3)}$$

The transmittance can be recast into an absorbance (equation S4) where the factor 2.303 connects the exponential expressed in equation S3 to the log to the base 10 in equation S4.

$$A_\lambda = -\log(\frac{I}{I_o}) = \frac{C_{ext}(\lambda)S}{2.303} \tag{S4}$$

The heat input from absorbing particles[16] is given by equation S5 where $P_o$ is the laser power, η is the efficiency of converting absorbed light into heat (for gold NPs, η is 1), and $A_\lambda$ is the wavelength dependant absorbance with $A_\lambda = \frac{C_{abs}(\lambda)S}{2.303}$. The extinction cross section has been replaced with an absorption cross section because only absorbed light is converted into heat.

$$q(W) = P_o(1-10^{-A_\lambda})\eta = 2.303P_oA_\lambda \tag{S5}$$

Equation S5 can be recast into $q(W) = nC_{abs}I_o$ using $I_o = \frac{P_o}{A_L}$ and $n = SA_L$ where $I_o$ is the laser intensity, $A_L$ is the laser area, and n is the total number of particles within the laser area. If n is one (single particle) then equation S6 results.

$$q(W) = C_{abs}I_o \tag{S6}$$

The local temperature around a heated NP is calculated using the thermal diffusion equation (S7) under the steady-state conditions:

$$\nabla k(\mathbf{r})\nabla\Delta T(\mathbf{r}) = -Q(\mathbf{r}) \tag{S7}$$

where the heat source is due to the heat released by a NP. If the thermal conductivity (k) is a constant then the steady-state temperature change for a spherically symmetric heat source is given by equation S8 for r greater than or equal to the nanoparticle radius ($R_{NP}$).[16-18, 51, 52] Combining equations S6 and S8 gives equation S9 where the maximum temperature change is at the nanoparticle surface ($r = R_{NP}$). Equation S9 gives the relationship between maximum temperature change and absorption cross section.

$$\Delta T(r) = \frac{q(W)}{4\pi k_o r} \tag{S8}$$

$$\Delta T_{\max}(r = R_{NP}) = \frac{q(W)}{4\pi k_o R_{NP}} = \frac{C_{abs}I_o}{4\pi k_o R_{NP}} \tag{S9}$$

The relationship between temperature change and absorption cross section can be verified by starting the derivation from the absorption of light by a single spherical particle. For this case, the heat input per unit volume is given by equation (S10)[16-18, 51, 52] where $\omega = \frac{2\pi c}{\lambda}$, $E_o^2 = \frac{I_o 8\pi}{c\sqrt{\varepsilon_m}}$, $\varepsilon_m$ is the dielectric constant of the surrounding medium, $\varepsilon_{NP}$ is the dielectric constant of the NP, and $\varepsilon''_{NP}$ is the imaginary component of the NP dielectric constant.

$$Q(\frac{W}{m^3}) = \frac{\omega E_o^{\,2}}{8\pi}\left|\frac{3\varepsilon_m}{2\varepsilon_m + \varepsilon_{NP}}\right|^2 \varepsilon''_{NP} \tag{S10}$$

The heat generated per volume (equation S10) can be used to determine the total amount of heat

production (equation S11) by substituting $\omega = \frac{2\pi c}{\lambda}$ and $E_o^2 = \frac{I_o 8\pi}{c\sqrt{\varepsilon_m}}$ into equation S10 and multiplying by the nanoparticle volume. The absorption cross section can be solved if equation S11 is substituted into equation S6 for a single particle. The relationship between absorption cross section and temperature change is in agreement with equation S2. It should be noted that in this derivation we are using the electric dipole approximation for the extinction cross section[27, 49, 50] and assuming a zero scattering cross section. These approximations have been shown to be reasonably for particles 40 nm in diameter or less.[28] We will use equation S9 to determine the absorption cross from a temperature change once the thermal conductivity, laser intensity, and NP size are known. Conversely, if the absorption cross section of the NP is known, then the maximum temperature change can be determined if the above parameters are specified.

$$q(W) = \frac{24\pi^2 {R_{NP}}^3 {\varepsilon_m}^{3/2}}{\lambda} \left\{ \frac{\varepsilon''_{NP}}{(\varepsilon'_{NP} + 2\varepsilon_m)^2 + {\varepsilon''_{NP}}^2} \right\} I_o \qquad \text{(S11)}$$

**Characterization of nanostructures**

The photoluminescence spectrum from a hot and cold region of the temperature image is shown in figure S1. The spectrum (shown in black) is taken from a hot region of the temperature image. The peak height at 540 nm is larger than the peak height at 565 nm. Hotter temperatures increase the photoluminescence intensity of the higher energy peak at 540 nm relative to the lower energy peak at 565 nm. Colder temperatures reverse this trend and the photoluminescence intensity of the peak at 565 nm gains intensity relative to the peak at 540 nm.

Figure S2 is a AFM image of single 40 nm gold NPs on the $Al_{0.94}Ga_{0.06}N:Er^{3+}$ film. The red line is a profile taken across two NPs and is shown in the bottom of the figure. The height of the profile shows that the particles are single particles while the roughness is the baseline reveals the grain size of the $Al_{0.94}Ga_{0.06}N$ film.

Figure S3 are scattering spectra of single gold NPs and nanodots. The spectra were obtained by subtracting background scattering away from the nanostructure and then dividing by the spectral profile of the white light excitation source. The spectra have been scaled in intensity so that they can be displayed on the same graph.

Figure S4 is the calibration of our thermal sensor with temperature. The temperature of the thermal sensor was changed using a Peltier heater, and the photoluminescence spectrum from the thermal sensor collected as a function of laser intensity. The area under the curve attributed to the $^2H_{11/2}$ energy transition peak was determined and labeled peak area X1. The area under the curve attributed to the $^4S_{3/2}$ energy transition peak was determined and labeled peak area X2. The peak areas were baseline corrected to yield the emission only from the $^2H_{11/2}$ and the $^4S_{3/2}$ transitions. A plot of the natural log of the ratio X1/X2 versus 1/T yields a straight line. The slope (87 meV) is related to the energy difference between the transitions. Our calibration is over a limited temperature range, but this relationship has been shown to be linear for a much larger temperature range (ref). The data taken at different laser intensities is not superimposable because the laser heats the substrate and the thermal sensor film. The amount of heating increases with laser intensity but is constant for a given laser intensity. This heating introduces a temperature offset in our calibration. However, the thermal sensor is still able to measure a reliable increase in temperature above this offset. In our measurements we fix the y-intercept in

our calibration so that a plot of the background temperature as a function of laser intensity has a limit equal to the ambient laboratory temperature at zero laser intensity.

Figure S5 the temperature difference for the nanodots collected with different fibers as the laser intensity is varied. The same dot was interrogated in each case. The slope of the plot of temperature difference versus laser intensity increased by a factor of 1.7 for every factor of 2 decrease in the bore size of the collection fiber. The increase in the temperature of 1.7 is attributed to a decrease in the collection volume on the surface when the fiber bore size is decreased. This trend indicates that the image size of the hot spot created around the optically-excited nanostructure is much smaller than the collection volume at the surface.

Figure S6 is a histogram of the maximum temperature change of 40 nm gold NPs optically-excited with a laser intensity of 5 x $10^{10}$ W/m$^2$, a 50x dark-field objective, and a 50 μm optical fiber. The histogram is fitted with a log-normal distribution. The average maximum temperature change of a single 40 nm gold nanoparticle is 15 K.

Figure S7 shows the characteristic dimensions of the gold nanodots fabricated with e-beam lithography with lift-off. Atomic force microscopy (AFM) studies give the height of the nanodots to be ~ 71 nm, and scanning electron microscopy (SEM) studies show that the diameter of the nanodots is ~ 120 nm. The total volume of the nanodots provides an effective radius of ~ 60 nm.

Figure S8 is an AFM image of a small segment of the nanodot array. The line profile across a row of the array shows that the height in the nanodots varied from 62 nm to 75 nm. The average height with uncertainty at the 95% confidence interval is 71 ± 3.5 nm.

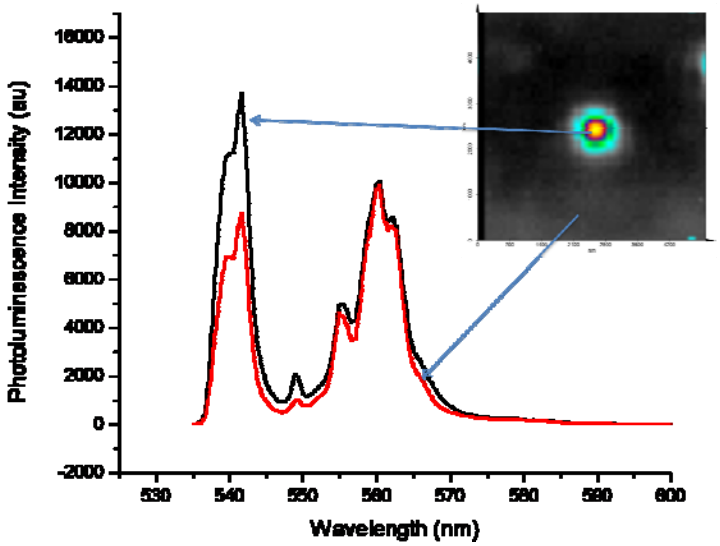

Figure S1.

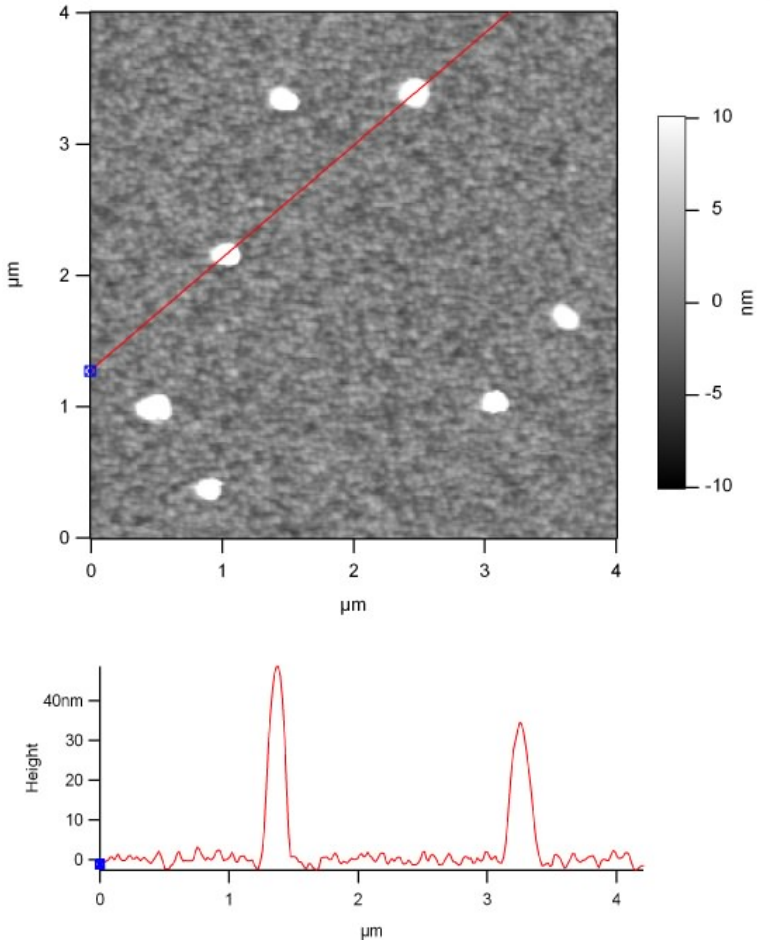


Figure S2.

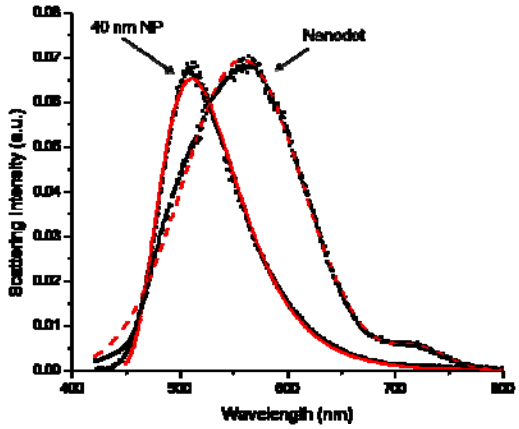


Figure S3.

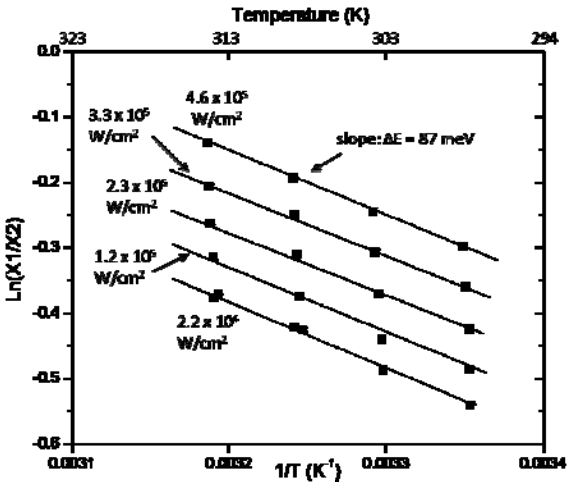


Figure S4.

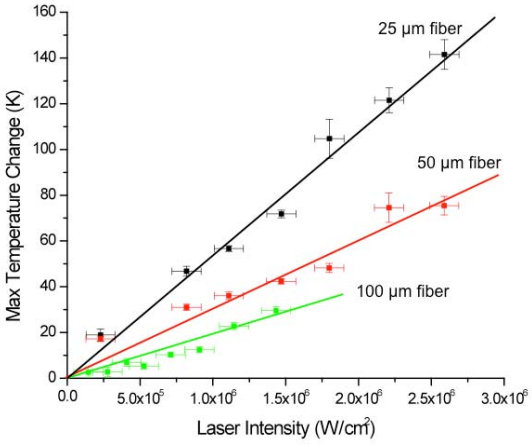


Figure S5.

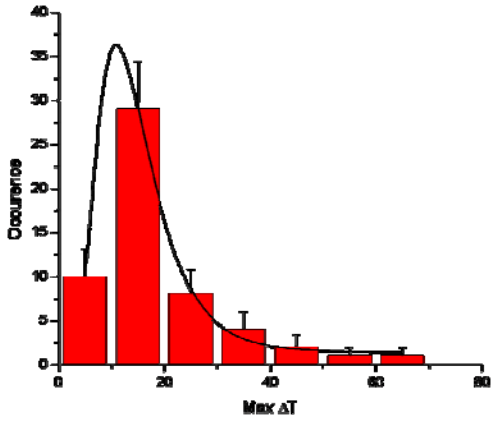


Figure S6.

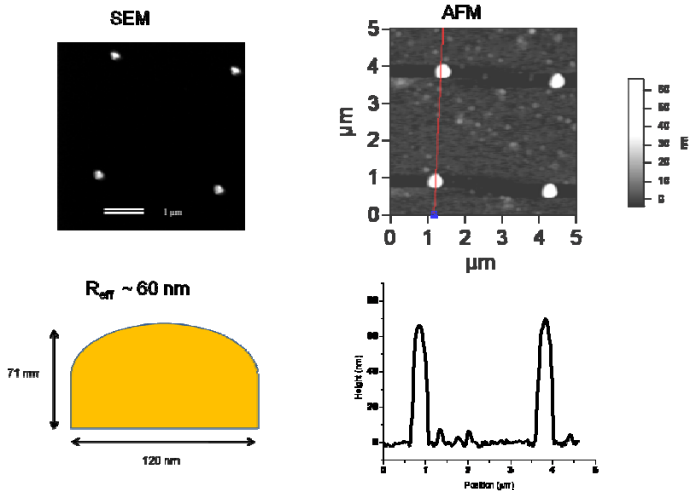


Figure S7.

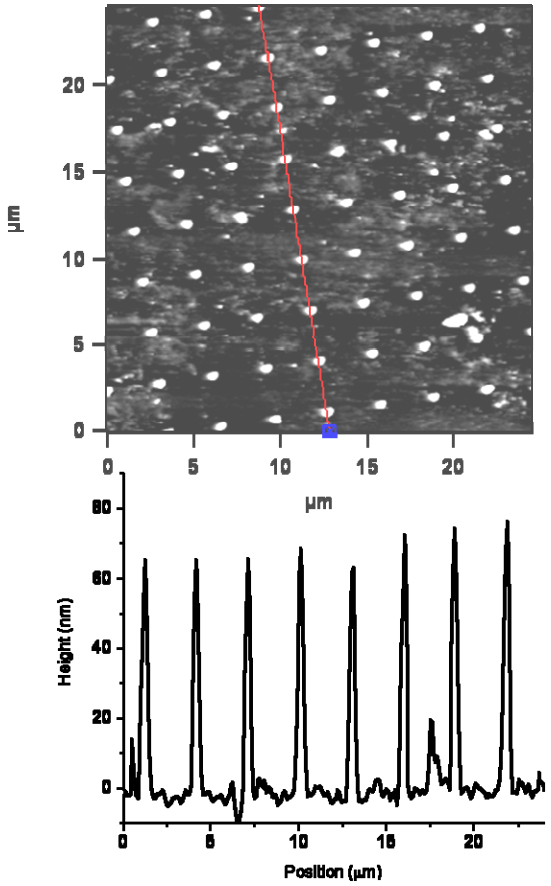


Figure S8.